Polymer 131 (2017) 104–110

Contents lists available at ScienceDirect

Polymer

journal homepage: www.elsevier.com/locate/polymer

Linear rheology of polymer nanocomposites with polymer-grafted nanoparticles

Marissa Giovino [a, *], Julia Pribyl [b], Brian Benicewicz [b], Sanat Kumar [c], Linda Schadler [a]

[a] Department of Materials Science and Engineering, Rensselaer Polytechnic Institute, Troy, NY 12180, United States
[b] Department of Chemistry and Biochemistry, University of South Carolina, Columbia, SC, 29208, United States
[c] Department of Chemical Engineering, Columbia University, New York, NY, 10025, United States

ARTICLE INFO

Article history:
Received 31 July 2017
Received in revised form
3 October 2017
Accepted 7 October 2017
Available online 9 October 2017

Keywords:
Polymer nanocomposite
Rheology
Composite viscosity

ABSTRACT

Polymer nanocomposites with polymer grafted nanoparticles (NPs) are of great interest since they have improved properties relative to their unfilled analogs. While it is well-appreciated that nanocomposite flow behavior is critically affected by filler dispersion, the roles of the matrix and the polymeric grafts remain unexplored. We perform linear oscillatory rheology on composites of polystyrene-grafted silica NPs in two different polystyrene matrices which have similar dispersion states and glass transition temperatures, T_g. When the matrix viscosity is considerably lower than that of the neat NP melt, the composite viscosities follow the scaling ideas applicable to star/linear polymer mixtures, well above the Einstein prediction. The higher matrix molecular weight shows lower viscosity, essentially following the Einstein relationship, presumably because faster modes of relaxation become available. We conclude that there is a deep, currently unexploited, analogy between the viscosity of polymer-grafted NP and star polymers.

© 2017 Elsevier Ltd. All rights reserved.

1. Introduction

Polymer nanocomposites often have improved mechanical [1–4], optical [5,6], thermal and electrical properties [7–9] over their unfilled polymer counterparts. The filler size, distribution and dispersion can change each of those properties significantly [10–13]. While it is generally believed that materials with well-dispersed fillers have enhanced properties [14], our work on the rheology of the melt state reveal that mechanical reinforcement is maximized when the particles percolate across the system, a result that is most easily attained when the NPs form highly anisotropic assemblies.

Our previous work has shown that the NP dispersion state can be controlled by varying the density and chain length of polymer grafts on the NP surface [13]. The idea here is that the NP and the polymer grafts are immiscible, and hence the surfactancy of these materials can be varied by altering the graft parameters. A newer idea is that the effective attraction between the NP cores, or alternately the repulsion between the cores and the polymeric coronas, can be controlled with fillers bearing two populations of polymer brushes: a densely grafted short brush which reduces the effective attraction between NP cores and a sparsely grafted long brush which controls the entropic interactions (and miscibility) with the matrix [14–16].

While there has been considerable interest in the viscosity behavior of grafted brush nanocomposites, there is currently no method for predicting this quantity as a function of graft density and molecular weight of the brush and matrix molecular weight. Much of the current understanding, experiments and simulations are limited to bare fillers or short brush grafted fillers ($M < M_e$) in a polymer melt. Nanocomposite viscosity has been shown to be a complex function of particle size and matrix molecular weight [17–24]. It has been found that adding small polystyrene beads to polystyrene matrices of different molecular weight can result in composites with higher or lower viscosity than the polymer melt [18–22,25–27]. Computer simulations [17,23,24,27–29] show several regimes of plasticization (lowered viscosity) and reinforcement (increased viscosity) [17]. For short unentangled matrix chains, plasticization occur for fillers with a diameter less than R_g, the chain radius of gyration. For long matrix chains, plasticization is found for fillers with size smaller than the entanglement tube diameter, i.e., $2R < d_T$ [30]. All of these effects are predicted in the case of athermal mixtures; the introduction of attractions between

* Corresponding author.
E-mail address: giovim@rpi.edu (M. Giovino).

https://doi.org/10.1016/j.polymer.2017.10.016
0032-3861/© 2017 Elsevier Ltd. All rights reserved.

the NPs and the chains serve to shift these boundaries so that it becomes harder to see regimes with reduced viscosities on the addition of the NPs. The available experimental data fit well within these predicted regimes. However, these simulation studies did not comment on the increase of free volume with the addition of nanoparticles and they were limited to bare fillers and very low filler loadings.

To the best of our knowledge, the viscosity of nanocomposites with long brush grafted fillers has yet to be systematically investigated. One aspect that is well-appreciated is that the NP dispersion state strongly controls the rheology of these materials. Thus, solid-like mechanical response at low frequencies, i.e., a plateau in G′ as a function of frequency, occurs when the NPs percolate across the system, with this percolation being controlled by the grafting density, chain length and the matrix length. While this knowledge exists, the consequences of the graft parameters on the viscosity of the nanocomposites and the parameters that control them remain unexplored at this time. In this paper, we examine the viscosity of polystyrene-grafted SiO_2 nanoparticles well dispersed in two homopolymer matrices to understand these issues.

An important background study, which will be of relevance, is how the viscosity of mixtures of star and linear polymers vary with the star functionality, and the zero-shear viscosity of the linear chains. Struglinksi et al. [31] found that the blend's zero shear viscosity, η_0, was dependent on the viscosities of the individual components, namely $(\eta_0)_1$ and $(\eta_0)_2$ as:

$$\eta_0 = (\eta_0)_1^{\phi_1} \times (\eta_0)_2^{\phi_2} \quad (1)$$

where ϕ_1 is the volume fraction of component 1, as long as the star's viscosity was much larger than that of the neat melt [31]. The situation where the melt has a higher viscosity than the star was probed indirectly by Watanabe et al. [32] who found that the star relaxation in these cases was much faster than that expected by diffusion if it followed the Stokes-Einstein relationship, i.e., if it was directly determined by the macroscopic viscosity of the blends.

Here, we critically examine the applicability of these ideas to the nanocomposite systems of our interest. We show that for systems with good NP dispersion, the matrix molecular weight plays a critical role in determining the system's viscosity behavior. When the matrix molecular weight is comparable to the molecular weight of a polymer graft, the viscosity follows Eq. (1). In contrast, when the matrix molecular weight is doubled, Eq. (1) dramatically overpredicts the system viscosity, which instead follows the Einstein relationship with the NP playing the role of a colloidal particle.

2. Experimental

SiO_2-7k-100k Synthesis: Bimodal brush particles were synthesized using a sequential RAFT polymerization similar to a process described previously [14]. To a solution of colloidal silica particles (Nissan Chemicals Inc., 30 wt% dispersion in MIBK, SiO_2 density = 2.2 g/mL) diluted with THF, we added 3-aminopropyldimethylethoxysilane and a trace amount of octyldimethylmethoxysilane to maintain dispersibility through this synthetic step. This mixture was heated at 65° C for 4 h under an inert (N_2) atmosphere. The surface-anchored amine groups were then allowed to react with 2-mercaptothiazoline-activated 4-cyanopentanoic acid dithiobenzoate (CPDB). The graft density of these covalently bound chain transfer agents was determined by comparing a UV-Vis spectrum of a grafted particle sample dispersed in THF to a calibration curve constructed from known amounts of free CPDB in solution. The surface polymerization of styrene monomer was performed at 65° C. The polystyrene-grafted particles were precipitated in hexane and recovered by centrifugation. The chains from a small sample of polystyrene-grafted particles were cleaved using hydrofluoric acid (HF), and the chain length and dispersity were analyzed by gel-permeation chromatography (GPC). The remainder of the sample was redispersed in THF. A large excess of azobis(isobutyronitrile) (AIBN) was used to cleave the RAFT agent to prevent further chain growth.

The particles, grafted with the short brush of polystyrene, were refunctionalized with CPDB as described above. A small sample of these particles was vacuum dried for TGA and UV-Vis analysis. The graft density of the second population of chain transfer agent was determined by normalizing the % silica in the sample based on TGA weight loss due to grafted polystyrene, and this corrected mass was correlated with the UV-Vis spectrum of the sample to determine the density of RAFT agents on the silica surface. The polymerization of this second population of polystyrene chains was conducted as described above. After the polystyrene-grafted particles were precipitated in hexane, a small sample was taken and the chains cleaved with HF. The molecular weight and dispersity of both populations of cleaved chains was analyzed by GPC. The bimodal polymer grafted particles were redispersed in THF, and the second population of RAFT agent was cleaved using a large excess of AIBN before further use.

In the rest of this study we used a filler which was a 15 nm diameter silica termed SiO_2-7k-100k. Two populations of polymer brushes were grafted to the surface: a short polystyrene brush with MW = 7 kg/mol and a graft density = 0.25 chains/nm^2, and long polystyrene brush with MW = 100 kg/mol and a graft density = 0.08 chains/nm^2.

Composite Processing: The matrix polymers (96 kg/mol or 190 kg/mol polystyrene) were individually dissolved in THF to make a 0.1 g/mL solution. The PS grafted SiO_2 nanoparticles were added to this solution to generate specific loadings. The volume percent of SiO_2 were: 1 vol%, 2 vol%, 3 vol% and 4 vol%, respectively. The solution was mixed using a Sonics and Materials Vibracell VCX 750 Watt unit for 1 min at 40% amplitude using the pulsed setting of 2 s on and 0.5 s off. The solution was cast at room temperature into aluminum boats. The composites were annealed in a vacuum oven at 120° C for 1 day and 18 h, and then hot pressed at 140° C in a Carver hot-press. Another set of samples at 2 vol% SiO_2 in 96k and 190k PS was prepared in the same way and annealed for 7 days. It was found that the samples annealed for 7 days had similar dispersion states, glass transition temperatures, viscosity data and shear modulus data to the samples annealed for the shorter times. This suggests, the samples annealed for ~2 days were near equilibrium.

Rheology: Oscillatory rheology experiments were conducted on a TA instruments AR-G2 rheometer with parallel plate geometry. A strain sweep was run at 1 rad/s to determine the linear viscoelastic region. Frequency sweeps were run at 1.5% strain from 250 rad/s to 0.25 rad/s. Normalized viscosity was calculated by dividing composite zero shear viscosity (η_0) by matrix polymer η_0. The polystyrene grafted nanoparticle viscosity was approximated as the viscosity of hot pressed polystyrene grafted SiO_2 discs at the highest temperature and lowest frequency.

3. Results and discussion

The TEM images in Fig. 1 show that the nanoparticles are well dispersed throughout the matrix for all loadings in both matrices. A more quantitative metric of dispersion is the mean free length L_f [33], which is the measure of the filler free or pure polymer domain size. For well dispersed samples L_f can be thought of as interparticle distance. For a given volume fraction of filler and for a fixed sample slice thickness, a smaller L_f is indicative of a better dispersion.

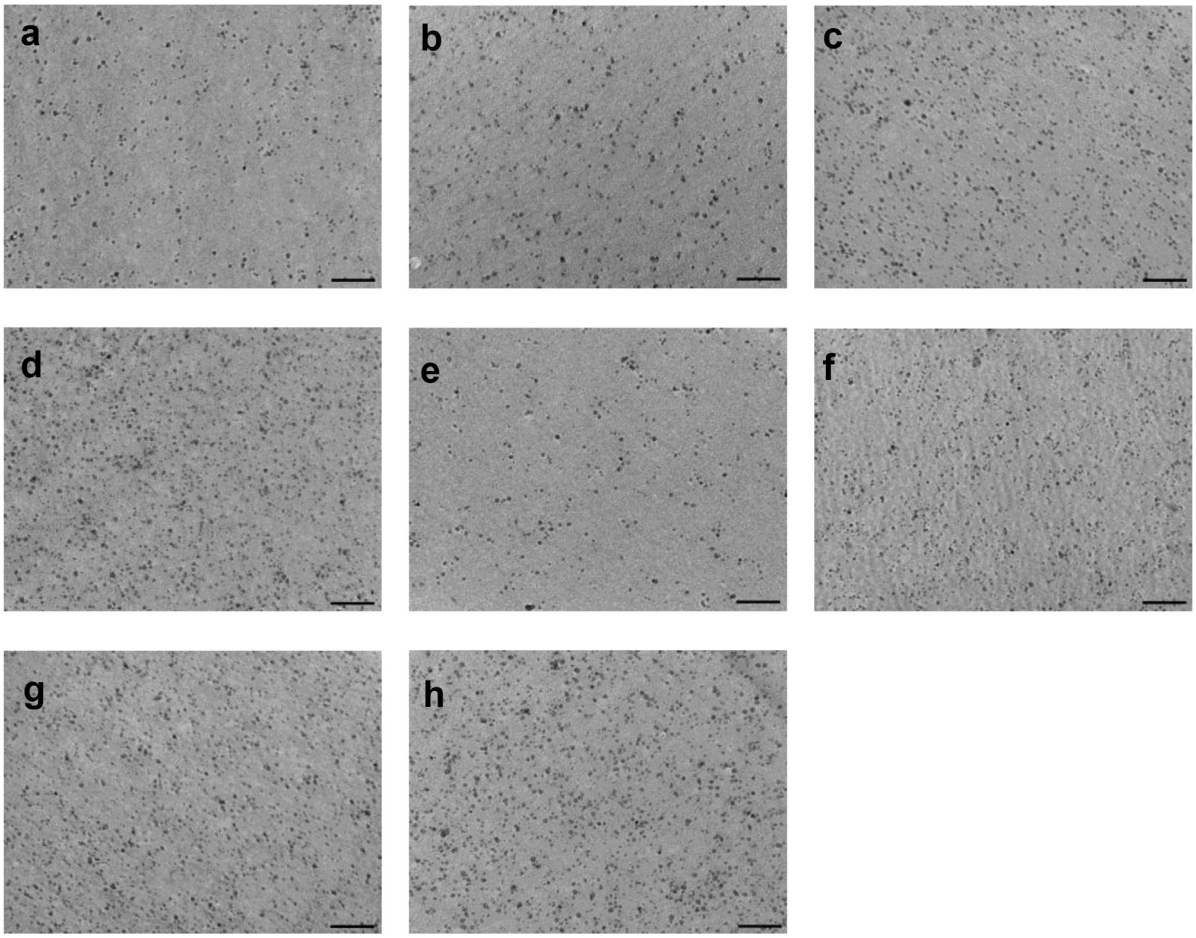

Fig. 1. TEM images of SiO_2 7k 100k polystyrene composites. All scale bars are 200 nm a-d) 1 vol%, 2 vol%, 3 vol% and 4 vol% SiO_2 in 96k PS. e-h) 1 vol%, 2 vol%, 3 vol% and 4 vol% SiO_2 in 190k PS.

Table S1 in the supporting information lists the L_f for the four loadings in each matrix. For a given loading, L_f is similar for the 96k matrix and 190k matrix and at both annealing times indicating that the dispersion state is similar. Given that we have four different loadings we have deduced the scaling of L_f with the silica loading in the sample, ϕ_{silica}, as $L_f \sim \phi_{silica}^{-2/3}$. The prefactor here turns out to 7 nm, which is comparable to the radius of the NPs. Why we obtain this precise scaling is unclear to us, and we leave this as an open question at this time. Nevertheless, both materials display excellent nanoparticle dispersion.

The thermal properties of the matrix polymer and polymer nanocomposites were measured using Differential Scanning Calorimetry (DSC). As filler loading increased, the glass transition temperature (T_g) decreased as seen in Fig. 2. To further explore the thermal behavior of these materials, the T_g of a composite with only brush modified nanoparticles was measured and found to be 100.8° C ±0.5° C. We compare our experimental results with predictions of the Fox-Flory equation:

$$\frac{1}{T_g} = \frac{w_1}{T_{g,1}} + \frac{w_2}{T_{g,2}} \tag{2}$$

where T_{gx} is the T_g of component x and w_x is its weight fraction. In this case, component 1 is the matrix polymer and component 2 is the polymer grafted filler. The predictions of this equation are shown in Fig. 2 and the error bars represent the standard deviation in the T_g measurement. The 96k matrix composites matches the Fox equation prediction up to 0.24 wt fraction of filler plus grafted polymer. The 190k matrix composites match up to 0.08 wt fraction of filler plus grafted polymer and shows a negative deviation at higher loadings. This suggests better mixing between the grafted and matrix chains in the 96k PS composites than in the 190K composites. Thus, while these systems always show good NP dispersion, these results indicate that the entropic penalty for matrix/brush mixing is beginning to become important for the larger matrix molecular weight.

The flow behavior of these materials was measured by linear oscillatory rheology. The relative viscosity (η_{rel}), i.e., the composite's zero shear viscosity (η_0) normalized by the matrix's zero shear viscosity, is plotted against filler loading (ϕ) for the two sets of composites in Fig. 3. Because the T_g varies in these samples (and thus the free volume at a constant temperature), it is important to compare the viscosity at the same homologous temperature (T_h) defined for pure matrix polymer as: $T_h = \frac{T}{T_g}$. This homologous temperature and the composite T_g were then used to determine the measurement temperature for the viscosity. The experimental data measured at constant temperature is shown in Figure S1. The trends in Figure S1 are similar to those adjusted for the homologous

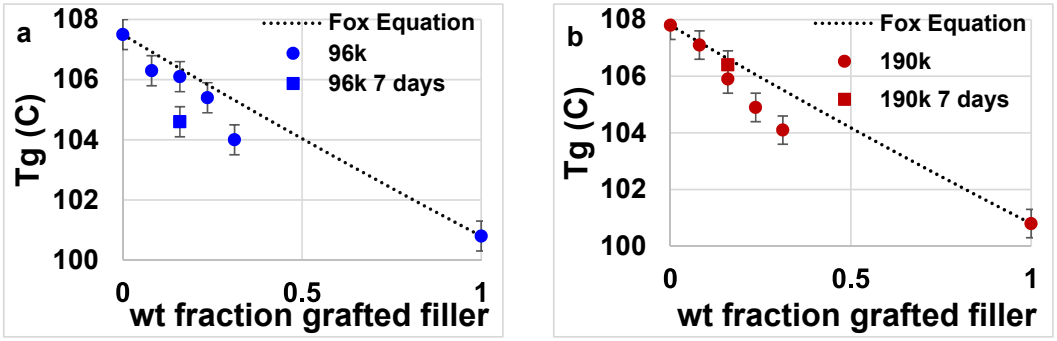

Fig. 2. Glass transition temperature for each composite set and theoretical prediction from Fox equation. a) thermal data for 96k PS matrix composites. b) thermal data for 190k PS matrix composites.

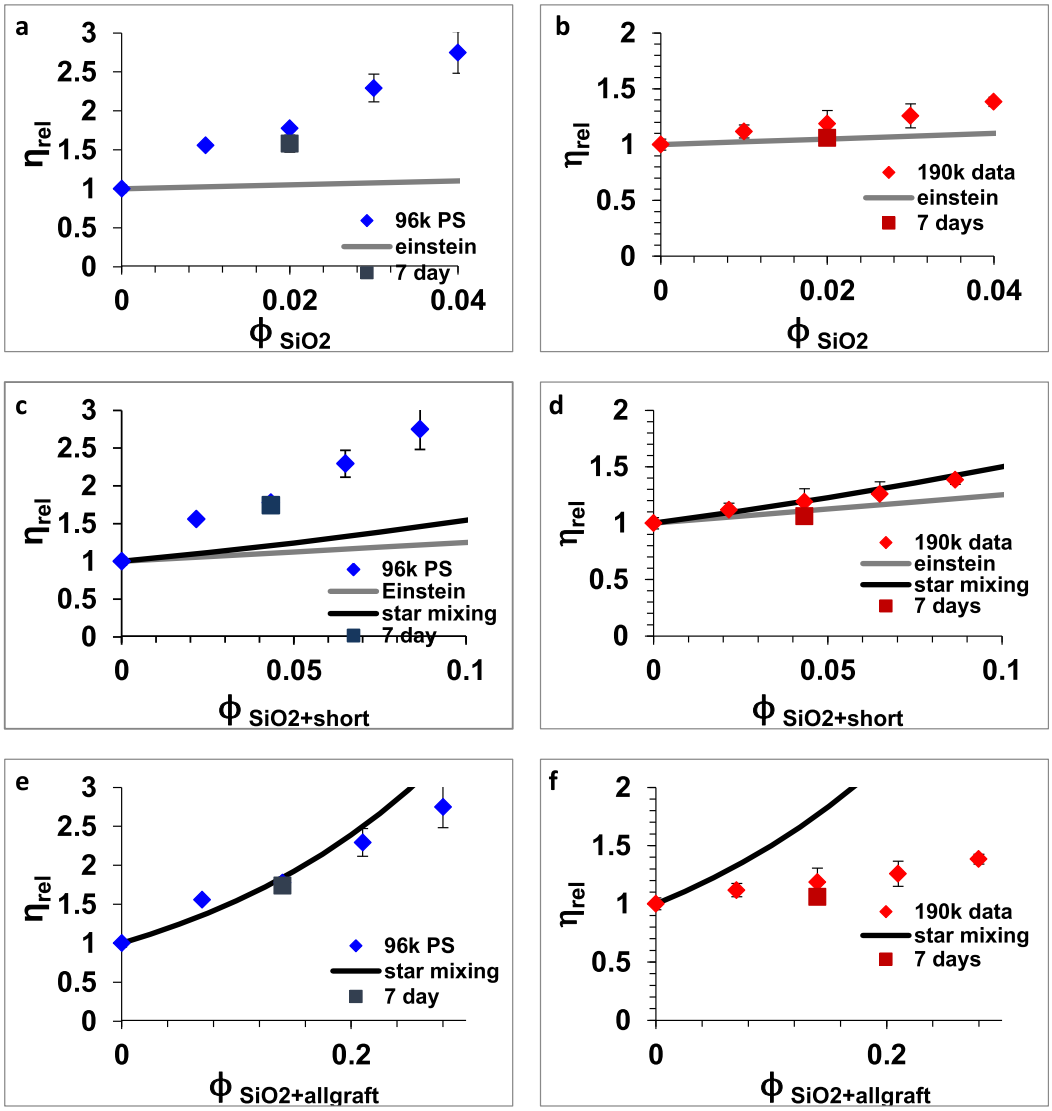

Fig. 3. Relative viscosity vs. filler loading plots measured at Th. A) Normalized zero shear viscosity vs loading of SiO_2 for 96k PS. B) Normalized viscosity verses loading of SiO_2 for 190k PS. C) Normalized zero shear viscosity vs loading of SiO_2 and short grafted polymer for 96k PS. D) Normalized viscosity verses loading of SiO_2 and short grafted polymer for 190k PS. E) Normalized zero shear viscosity vs loading of SiO_2 and grafted polymer for 96k PS. F) Normalized viscosity verses loading of SiO_2 and grafted polymer for 190k PS.

temperature (Fig. 3). In Fig. 3a and b the Einstein prediction for the viscosity, $\eta_{rel} = 1 + 2.5\phi$, is shown for comparison. The largest deviation from Einstein's prediction is seen in the 96k PS matrix composites. There is a slight positive deviation from the Einstein prediction in Fig. 3b (190k); the addition of the quadratic term does not help in bringing better agreement. In Fig. 3c and d the short brush is added to the volume fraction of the filler. In this case there is a large positive deviation for the 96k PS matrix and for the larger 190k PS matrix the data is close to both the batchelor model and the star mixing model. The two sets of composites have the same particle distribution as verified by TEM images and L_f calculations, grafted filler (SiO_2-7k-100k), processing conditions and experimental setup. The only difference between the two is the matrix polymer molecular weight. The interactions between the matrix polymer and grafted polymer are therefore conjectured to cause different deviations from the Einstein equation.

In contrast to the results presented above, it is seen that the 190k data set in Fig. 3e is not fit well by the star polymer model (Eq. (1)) for any loading. However, the 96k matrix data, in Fig. 3f, is fit well by this equation at loadings up to 20 vol%. Since the viscosity of the PS grafted SiO_2 NPs is about ~600 times larger than for the 96k matrix but only ~60 times larger than the 190k matrix, it is reasonable that the former data indeed conform to the predictions of the star/linear mixtures ideas proposed by Struglinski et al. [31] We thus conjecture that the higher molecular weight matrices are thus in a regime where some other relaxation process, such as dynamic dilution, is occurring which leads to faster relaxations and hence lower than expected viscosities. This conclusion is consistent with the T_g results which suggest that the 190k samples had a lower than expected glass transition temperature, or faster segmental dynamics. These findings are also consistent with results published for solid state composites. Natarajan et al. investigated the stiffness of polymer nanocomposites by nanoindentation [14]. A larger normalized stiffness was found for polymer nanocomposites with a grafted brush MW similar to the matrix MW. Fracture behavior was found to change with matrix MW [34]. For grafted polymer of low MW, brittle failure in the form of crazing was observed; for high MW grafted polymer, shear bands were observed [34].

To gain more insight into the polymer nanocomposite melt behavior, their shear moduli were measured via oscillatory rheology. Master curves were generated from time temperature superposition data for each sample. The shear storage modulus master curves are shown in Fig. 4. There is no significant change in the rubbery plateau (at intermediate frequencies) with filler loading for either set of composites. The rubbery plateau modulus, $G_{N,}$ is related to the entanglement molecular weight M_e [35].

$$G_N = \frac{\rho RT}{M_e} \tag{3}$$

Since G_N is constant for all loadings this suggests that the filler has not measurably changed the M_e (e.g. hasn't disrupted the entanglement network), a result that is consistent with computer simulations. There is, however, some change in the shear storage modulus in the low frequency terminal region.

Interesting trends in chain relaxation are seen in the terminal region. The slopes of the shear storage modulus in the terminal region are a qualitative measure of the polymer chain relaxation times. A polymer melt is known to have a slope of two in this region. The terminal region experimental data and the corresponding slopes are shown in Fig. 5. For the 96k PS matrix composites in Fig. 5a, there is a noticeable decrease in the slope of G′ as filler loading is increased. This suggests that the filler is slowing the chain relaxation in these composites. In Fig. 5b the data for the 190k PS matrix set is shown. Here there a smaller decrease in slope as filler loading is increased, indicating the chain relaxation is faster in the 190k composites compared to the 96k composites at the same filler loading.

4. Discussion

There are essentially three results that have emerged from this work: (i) All the nanocomposites studied show a negative deviation from the Fox-Flory equation for T_g, with this departure occurring at lower volume fractions for the larger molecular weight matrix. (ii) The viscosity of the nanocomposite with the low molecular weight matrix follows empirical ideas developed for star/linear polymer blends. (iii) The viscosity of the nanocomposite with the higher molecular weight blend appears to follow the Einstein relationship. We propose two alternative scenarios to explain these results:

Since the overall distance between the NPs has not changed when we vary the matrix molecular weight, and the number of entanglements has not changed, some other factor is leading to the change in T_g and the rheology behavior that we observe. One possibility is changes in miscibility of the system, which is determined by the ratio of matrix polymer to grafted polymer molecular weight or P/N [11,12,14–16,34]: it is known for relatively high grafting densities that phase separation occurs when P/N > 4, and the grafted brush will collapse. For our system the 96k matrix the P/N ratio is 0.96 whereas for the 190k matrix the P/N ratio is 1.9 [36–38], and so one possibility is that these systems are becoming less miscible with increasing matrix length [36,37,39]. This hypothesis simultaneously explains the larger T_g decreases and the departure of rheological behavior from star/linear melt like to an Einstein-like behavior found with the larger molecular weight matrices (Fig. 3b, d and 3f support this as the experimental data for 190k is closest to the Batchelor model which is valid for micron sized hard spheres.). The data in Fig. 3b show a small decrease in the terminal region slope with loading, for hard spheres we would

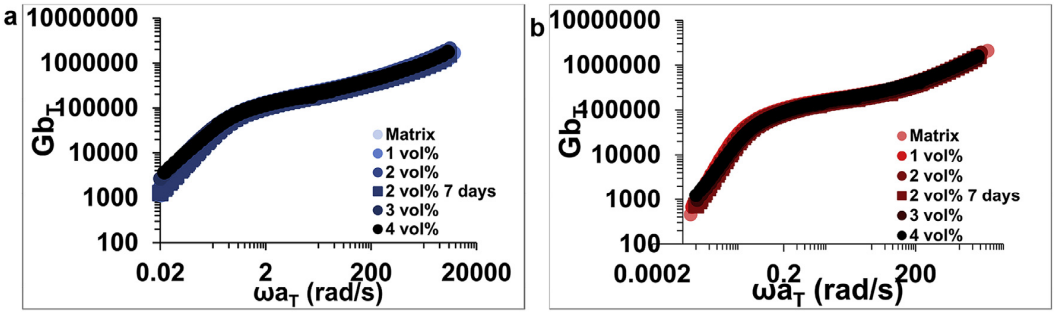

Fig. 4. Storage modulus master curves generated from Time-Temperature-Superposition. A) Master curves for composites in 96k PS. B) Master curves for composites in 190k PS.

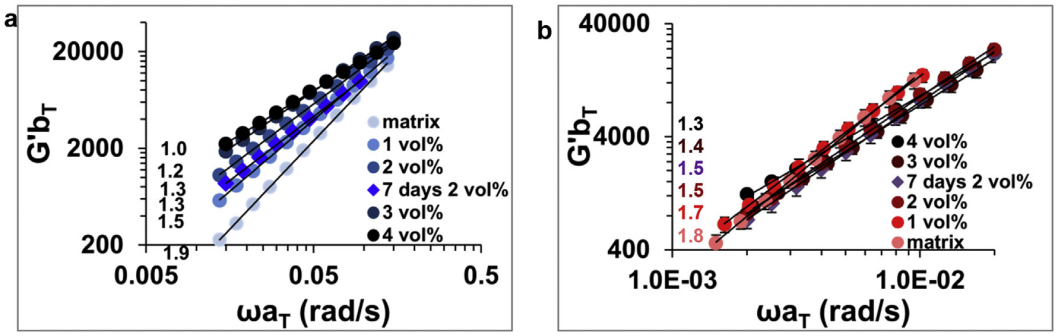

Fig. 5. Shear storage moduli terminal region for polymer nanocomposites. a) storage moduli for 96k PS matrix composites. b) storage moduli for 190k PS matrix composites.

expect little change in this slope until very high loadings ϕ~0.5.

While these conclusions appear reasonable at first glance, there is little evidence in the literature to support the claim that a reduced miscibility between the brush and the matrix manifests itself in measurable properties at these P/N values. Indeed Chevigny et al. [38], and Jayaraman, Krishnamoorti and coworkers have shown that brush dimensions do not change in the single phase regime, and measurable changes only occur in regimes where phase separation occurs, i.e., P/N > 4. Thus, unless the behavior is different in the case of bimodal grafts, we may need another mechanism to explain the rheological and thermal response of these blends. Thus, another possibility is the change in relaxation mechanism with increasing matrix chain length. For short matrices, the matrix relaxes much quicker than the grafted chains: the slowest relaxation therefore is the star-like relaxation of the tethered chains in an entanglement mesh formed by the grafted chains on adjacent stars. This behavior should result in viscosity behavior following that observed for star/linear mixture, in good agreement with the fact that the viscosity of these mixtures follow the Struglinski et al. ideas (Eq. (1)). With increasing matrix molecular weight, however, following Watanabe et al., we propose that the mode of relaxation changes from arm retraction to a constraint release Rouse like motion of the arms which is retarded due to the presence of the matrix. The fundamental point here is that the mechanism changes from something reminiscent of a star molecule to something more akin to the behavior of a colloidal particle in a polymer melt with increasing matrix molecular weight.

5. Conclusion

We explore the dynamic properties of polymer nanocomposites where good, uniform NP dispersion is achieved by grafting a bimodal brush on the NPs: a dense population of short grafted polymers reduces the enthalpic attraction between the NP cores, while a sparse second population provides the entropic drive for miscibility with the matrix. Oscillatory rheology was used to measure the viscosity and shear moduli for the two composite systems, where the NP was held constant but the matrix molecular weight was doubled from ~96k to 190k. The two composites had distinct viscosity behavior despite similar dispersion states, T_g and processing conditions. It was found that the viscosity of the composite with the 96k matrix acts similar to a star-linear mixture has slower chain relaxation. In contrast, the composites with the 190k matrix follow the Einstein equation suggesting that the NP acts akin to a colloidal filler in the polymer melt. More detailed investigations of this interesting transition behavior, as a function of matrix molecular weight are necessary to fully understand this very interesting behavior.

Conflict of interest

None.

Acknowledgements

We thank Prof Ryu for helpful discussions about rheology and polymer chain relaxation. This work was supported by the National Science Foundation [EEC-0812056] and by New York state under NYSTAR [C090145].

Appendix A. Supplementary data

Supplementary data related to this article can be found at https://doi.org/10.1016/j.polymer.2017.10.016.

References

[1] D. Shah, P. Maiti, D.D. Jiang, C.A. Batt, E.P. Giannelis, Effect of nanoparticle mobility on toughness of polymer nanocomposites, Adv. Mater 17 (2005) 525–528, https://doi.org/10.1002/adma.200400984.
[2] H. Zhang, Z. Zhang, K. Friedrich, C. Eger, Property improvements of in situ epoxy nanocomposites with reduced interparticle distance at high nanosilica content, Acta Mater 54 (2006) 1833–1842, https://doi.org/10.1016/j.actamat.2005.12.009.
[3] B. Wetzel, F. Haupert, M.Q. Zhang, Epoxy nanocomposites with high mechanical and tribological performance, Compos. Sci. Technol. 63 (2003) 2055–2067, https://doi.org/10.1016/S0266-3538(03)00115-5.
[4] X. Zhao, Q. Zhang, D. Chen, P. Lu, Enhanced mechanical properties of graphene-based polyvinyl alcohol composites, Macromolecules 43 (2010) 2357–2363, https://doi.org/10.1021/ma902862u.
[5] A. Dang, S. Ojha, C.M. Hui, C. Mahoney, K. Matyjaszewski, M.R. Bockstaller, High-transparency Polymer Nanocomposites Enabled by Polymer- Graft Modi Fi Cation of Particle Fillers, 2014.
[6] J. Kim, H. Yang, P.F. Green, Tailoring the refractive indices of thin film polymer metallic nanoparticle nanocomposites, Langmuir 28 (2012) 9735–9741, https://doi.org/10.1021/la300374w.
[7] J. Wang, J. Dai, T. Yarlagadda, Carbon nanotube - conducting-polymer composite nanowires, Langmuir 21 (2005) 9–12.
[8] Y. Geng, M.Y. Liu, J. Li, X.M. Shi, J.K. Kim, Effects of surfactant treatment on mechanical and electrical properties of CNT/epoxy nanocomposites, Compos. Part A Appl. Sci. Manuf. 39 (2008) 1876–1883, https://doi.org/10.1016/j.compositesa.2008.09.009.
[9] H. Gómez, M.K. Ram, F. Alvi, P. Villalba, E. Stefanakos, A. Kumar, Graphene-conducting polymer nanocomposite as novel electrode for supercapacitors, J. Power Sources 196 (2011) 4102–4108, https://doi.org/10.1016/j.jpowsour.2010.11.002.
[10] C. Chevigny, F. Dalmas, E. Di Cola, D. Gigmes, D. Bertin, F. Boué, J. Jestin, Polymer-grafted-nanoparticles nanocomposites: dispersion, grafted chain conformation, and rheological behavior, Macromolecules 44 (2011) 122–133, https://doi.org/10.1021/ma101332s.
[11] P. Akcora, S.K. Kumar, J. Moll, S. Lewis, L.S. Schadler, Y. Li, B.C. Benicewicz, A. Sandy, S. Narayanan, J. Ilavsky, P. Thiyagarajan, R.H. Colby, J.F. Douglas, "Gel-like" mechanical reinforcement in polymer nanocomposite melts, Macromolecules 43 (2010) 1003–1010, https://doi.org/10.1021/ma902072d.
[12] J.F. Moll, P. Akcora, A. Rungta, S. Gong, R.H. Colby, B.C. Benicewicz, S.K. Kumar, Mechanical reinforcement in polymer melts filled with polymer grafted nanoparticles, Macromolecules 44 (2011) 7473–7477, https://doi.org/

10.1021/ma201200m.
[13] P. Akcora, H. Liu, S.K. Kumar, J. Moll, Y. Li, B.C. Benicewicz, L.S. Schadler, D. Acehan, A.Z. Panagiotopoulos, V. Pryamitsyn, V. Ganesan, J. Ilavsky, P. Thiyagarajan, R.H. Colby, J.F. Douglas, Anisotropic self-assembly of spherical polymer-grafted nanoparticles, Nat. Mater 8 (2009) 354–359, https://doi.org/10.1038/nmat2404.
[14] B. Natarajan, T. Neely, A. Rungta, B.C. Benicewicz, L.S. Schadler, Thermomechanical properties of bimodal brush modified nanoparticle composites, Macromolecules 46 (2013) 4909–4918, https://doi.org/10.1021/ma400553c.
[15] Y. Li, P. Tao, A. Viswanath, B.C. Benicewicz, L.S. Schadler, Bimodal surface ligand engineering: the key to tunable nanocomposites, Langmuir 29 (2013) 1211–1220, https://doi.org/10.1021/la3036192.
[16] D. Sunday, J. Ilavsky, D.L. Green, A phase diagram for polymer-grafted nanoparticles in homopolymer matrices, Macromolecules 45 (2012) 4007–4011, https://doi.org/10.1021/ma300438g.
[17] J.T. Kalathi, G.S. Grest, S.K. Kumar, Universal viscosity behavior of polymer nanocomposites, Phys. Rev. Lett. 109 (2012) 1–5, https://doi.org/10.1103/PhysRevLett.109.198301.
[18] R. Mangal, S. Srivastava, L.A. Archer, Phase stability and dynamics of entangled polymer-nanoparticle composites, Nat. Commun. 6 (2015) 7198, https://doi.org/10.1038/ncomms8198.
[19] A. Tuteja, M.E. Mackay, S. Narayanan, S. Asokan, M.S. Wong, Breakdown of the continuum Stokes-Einstein relation for nanoparticle diffusion, Nano Lett. 7 (2007) 1276–1281, https://doi.org/10.1021/nl070192x.
[20] A. Tuteja, P.M. Duxbury, M.E. Mackay, Multifunctional nanocomposites with reduced viscosity, Macromolecules 40 (2007) 9427–9434, https://doi.org/10.1021/ma071313i.
[21] M.E. Mackay, T.T. Dao, A. Tuteja, D.L. Ho, B. van Horn, H.-C. Kim, C.J. Hawker, Nanoscale effects leading to non-Einstein-like decrease in viscosity, Nat. Mater 2 (2003) 762–766, https://doi.org/10.1038/nmat999.
[22] U. Yamamoto, K.S. Schweizer, Theory of nanoparticle diffusion in unentangled and entangled polymer melts, J. Chem. Phys. 135 (2011), https://doi.org/10.1063/1.3664863.
[23] J.T. Kalathi, U. Yamamoto, K.S. Schweizer, G.S. Grest, S.K. Kumar, Nanoparticle diffusion in polymer nanocomposites, Phys. Rev. Lett. 112 (2014) 108301, https://doi.org/10.1103/PhysRevLett.112.108301.
[24] U. Yamamoto, K.S. Schweizer, Microscopic theory of the long-time diffusivity and intermediate-time anomalous transport of a nanoparticle in polymer melts, Macromolecules 48 (2015) 152–163, https://doi.org/10.1021/ma501150q.
[25] M. McEwan, D. Green, Rheological impacts of particle softness on wetted polymer-grafted silica nanoparticles in polymer melts, Soft Matter 5 (2009) 1705, https://doi.org/10.1039/b816975f.
[26] D.L. Green, J. Mewis, Connecting the wetting and rheological behaviors of poly (dimethylsiloxane) -grafted silica spheres in poly (dimethylsiloxane) melts, Langmuir 22 (2006) 9546–9553.
[27] U. Yamamoto, K.S. Schweizer, Theory of nanoparticle diffusion in unentangled and entangled polymer melts, J. Chem. Phys. 135 (2011) 0–16, https://doi.org/10.1063/1.3664863.
[28] J.T. Kalathi, S.K. Kumar, M. Rubinstein, G.S. Grest, Rouse mode analysis of chain relaxation in polymer nanocomposites, Soft Matter 11 (2015) 4123–4132, https://doi.org/10.1039/c5sm00754b.
[29] Y. Li, M. Kröger, W.K. Liu, Nanoparticle effect on the dynamics of polymer chains and their entanglement network, Phys. Rev. Lett. 109 (2012) 1–5, https://doi.org/10.1103/PhysRevLett.109.118001.
[30] A. Tuteja, M.E. Mackay, C.J. Hawker, B. Van Horn, Effect of ideal, organic nanoparticles on the flow properties of linear polymers: non-einstein-like behavior, Macromolecules 38 (2005) 8000–8011, https://doi.org/10.1021/ma050974h.
[31] M.J. Struglinski, W.W. Graessley, L.J. Fetters, Effects of polydispersity on the linear viscoelastic properties of entangled polymers. 3. Experimental observations on binary mixtures of linear and star polybutadienes, Macromolecules 21 (1988) 783–789, https://doi.org/10.1021/ma00181a039.
[32] H. Watanabe, T. Sato, K. Osaki, Viscoelastic relaxation of Styrene–Butadiene diblock copolymer micellar systems. 2. Behavior in entangling, long polybutadiene matrices, Macromolecules 29 (1996) 113–118, https://doi.org/10.1021/ma951249h.
[33] H.S. Khare, D.L. Burris, A quantitative method for measuring nanocomposite dispersion, Polym. Guildf. 51 (2010) 719–729, https://doi.org/10.1016/j.polymer.2009.12.031.
[34] D. Maillard, S.K. Kumar, B. Fragneaud, J.W. Kysar, A. Rungta, B.C. Benicewicz, H. Deng, L.C. Brinson, J.F. Douglas, Mechanical properties of thin glassy polymer films filled with spherical polymer-grafted nanoparticles, Nano Lett. 12 (2012) 3909–3914, https://doi.org/10.1021/nl301792g.
[35] J.D. Ferry, Viscoelastic properties of polymers. http://www.scopus.com/inward/record.url?eid=2-s2.0-84870726203&partnerID=tZOtx3y1, 1980.
[36] M.J. a Hore, J. Ford, K. Ohno, R.J. Composto, Direct measurements of polymer brush conformation using small-angle neutron scattering (sans) from highly-grafted iron oxide nanoparticles in homopolymer melts, Macromolecules 46 (2013) 9341–9348, https://doi.org/10.1021/ma401975a.
[37] G.G. Vogiatzis, D.N. Theodorou, Structure of polymer layers grafted to nanoparticles in Silica– polystyrene nanocomposites, Macromolecular 46 (2013) 4670–4683, https://doi.org/10.1021/ma400107q.
[38] C. Chevigny, J. Jestin, D. Gigmes, R. Schweins, E. Di-Cola, F. Dalmas, D. Bertin, F. Boué, "Wet-To-Dry" conformational transition of polymer layers grafted to nanoparticles in nanocomposite, Macromolecules 43 (2010) 4833–4837, https://doi.org/10.1021/ma100858h.
[39] D.M. Trombly, V. Ganesan, Curvature effects upon interactions of polymer-grafted nanoparticles in chemically identical polymer matrices, J. Chem. Phys. 133 (2010), https://doi.org/10.1063/1.3493330.